



ELSEVIER

Contents lists available at ScienceDirect

Biochemistry and Biophysics Reports

journal homepage: www.elsevier.com/locate/bbrep

Construction of P-glycoprotein incorporated tethered lipid bilayer membranes



Fatih Inci^a, Umit Celik^b, Basak Turken^a, Hakan Özgür Özer^c, Fatma Nese Kok^{a,*}

^a Istanbul Technical University, Molecular Biology, Genetics and Biotechnology Program, 34469 Istanbul, Turkey

^b Istanbul Technical University, Metallurgical and Materials Engineering Department, 34469 Istanbul, Turkey

^c Istanbul Technical University, Physics Department, 34469 Istanbul, Turkey

ARTICLE INFO

Article history:

Received 11 March 2015

Received in revised form

25 May 2015

Accepted 29 May 2015

Available online 4 June 2015

Keywords:

Tethered lipid bilayer

P-glycoprotein

Drug–protein interactions

Statins

ABSTRACT

To investigate drug–membrane protein interactions, an artificial tethered lipid bilayer system was constructed for the functional integration of membrane proteins with large extra-membrane domains such as multi-drug resistance protein 1 (MDR1). In this study, a modified lipid (*i.e.*, 1,2-distearoyl-sn-glycero-3-phosphoethanolamine-N-[amino (polyethylene glycol)-2000] (DSPE-PEG)) was utilized as a spacer molecule to elevate lipid membrane from the sensor surface and generate a reservoir underneath. Concentration of DSPE-PEG molecule significantly affected the liposome binding/spreading and lipid bilayer formation, and 0.03 mg/mL of DSPE-PEG provided optimum conditions for membrane protein integration. Further, the incorporation of MDR1 increased the local rigidity on the platform. Antibody binding studies showed the functional integration of MDR1 protein into lipid bilayer platform. The platform allowed to follow MDR1–statin-based drug interactions *in vitro*. Each binding event and lipid bilayer formation was monitored in real-time using Surface Plasmon Resonance and Quartz Crystal Microbalance–Dissipation systems, and Atomic Force Microscopy was used for visualization experiments.

© 2015 The Authors. Published by Elsevier B.V. This is an open access article under the CC BY-NC-ND license (<http://creativecommons.org/licenses/by-nc-nd/4.0/>).

1. Introduction

Biosensing and biointerface technologies have recently offered new insights to measure and monitor drug–protein interactions in real-time [1,2]. It is often complicated to study membrane protein–ligand and membrane protein–membrane interactions *in vivo* and *in vitro* conditions due to many external and internal factors involved in cellular organization. Cell membrane mimicking platforms (*i.e.*, model membrane systems) such as bicelles [3], nanodiscs [4], liposomes [5], black lipid films [6], solid-supported bilayer lipid membranes (sBLMs) [7], and tethered bilayer membranes (tBLMs) [8], are employed to investigate the membrane proteins, and provide information on drugs/toxins and membrane proteins interactions *in vitro*. Particularly, tBLMs provide great impact and utility on membrane protein investigations, where lipid membrane is elevated from the support surface using a spacer molecule (*e.g.*, peptide or polymer) which elevate the lipid bilayer from the support surface [9]. Recently, long polymer-based spacer molecules have been utilized to provide viscoelasticity to tBLMs, where membrane spanning proteins are inserted [10,11]. These membrane models mimic cellular environment by providing a

reservoir section to preserve native structure of membrane proteins *in vitro*. In addition, they minimize surface roughness effects over membrane proteins that interfere to the durability and accuracy of the constructed membrane system. These model membrane platforms can also be characterized using various surface sensitive techniques, imaging tools, and electrochemical devices [12–14]. For instance, Surface Plasmon Resonance (SPR) is an optical method to monitor the binding events on the sensor surface by analyzing changes in refractive index parameter reflecting the amount of binding molecule in real-time [15]. Quartz Crystal Microbalance–Dissipation (QCM–D), on the other hand, is sensitive to mass accumulation on the surface, and simultaneously records changes in total mass in terms of resonance frequency (f) and dissipation (D) [16]. Dissipation parameter is also used to evaluate the viscoelastic properties of constructed layers in lipid membrane research [17]. For visualization studies, Atomic Force Microscopy (AFM) has been employed to assess and explore the topography of solid and viscoelastic surfaces including lipid bilayers in nanometric scale. AFM also provides insight in mechanical characteristics of constructed surfaces (*e.g.*, viscoelasticity and rigidity) and the interaction forces in lipid bilayer platforms [18].

P-glycoprotein, a product of the multidrug resistance gene (MDR1), is a transmembrane protein, which pumps various exogenous and endogenous toxic compounds out of the cell as a part of cellular defense mechanism [19,20]. Recent experiments also

* Correspondence to: Istanbul Technical University, Molecular Biology and Genetics Department, 34469 Maslak, Istanbul, Turkey.

E-mail address: kokf@itu.edu.tr (F.N. Kok).

showed that MDR1 protein has crucial role in cancer cells [21], nervous system [22], diabetic [23] and HIV-1 infected individuals [24]. Since MDR1 is essential for cellular defense mechanism, to evaluate the interactions of this protein with various drugs/toxins has significant impact for medical and pharmaceutical studies. Due to its large cytoplasmic domain, however, its functional integration requires a tBLM platform, which utilizes a long spacer molecule. Although short spacer molecules (e.g. tetra ethylene glycol) could be used for insertion of small membrane proteins or pore forming peptides such as gramicidin and melittin [25,26], proteins with large extra-membrane domains require longer spacers. Using long spacer molecules like polyethylene glycol-2000 (PEG-2000) [10,11,27,28], PEG-5000 [29], or oxazoline derivatives [30,31] were reported by several groups. Although some of these studies have focused on membrane construction and characterization, only small proteins (< 50 kDa) were inserted in the constructed tBLM [10,27], and large membrane protein incorporation has not been studied [11,28,29,32,33]. Only limited studies involve the incorporation of large proteins such as ATPase [31] and integrin $\alpha_{\text{IIB}}\beta_3$ [30] on tBLMs, and in both reports, oxazoline derivatives were used as spacer molecule. In addition, integration of integrin $\alpha_{\text{IIB}}\beta_3$ had been done using fluorescently labelled proteins, and no further examinations have been performed to demonstrate their interactions with antibodies or drugs. ATPase, on the other hand, has a large extra-membrane part with ATP hydrolysis activity and this large domain had been extended to the upper part of the tBLM to perform activity measurements. In our study, however, large extra-membrane domain of MDR1 should be situated in the reservoir produced by the spacer molecule, not in the upper part, since specific antibody and drug that were used would interact with the opposite side of the protein.

In our study, a tBLM platform was constructed on a solid support surface to integrate MDR1 (i.e., P-glycoprotein) by using a modified polymer spacer (PEG-2000-modified lipid molecule). To the best of our knowledge, there is no prior study that demonstrates functional incorporation of MDR1 protein with correct orientation, as well as evaluation of drug (i.e., statin) interactions with MDR1 protein on model membrane platforms. As a model drug, pravastatin, a cholesterol lowering drug, was utilized since it has been reported to interact with MDR1 protein and inhibits its function [34]. To characterize the platform, three different technologies, namely SPR, QCM-D, AFM in liquid, were employed.

2. Materials and methods

2.1. Materials

L- α -Phosphatidylcholine (PC) from egg yolk (P3556), 3,3'-dithiodipropionic acid di(N-hydroxysuccinimide) (DTSP) (D3669), pravastatin (P4498), P-glycoprotein (MDR1) (M9194), monoclonal anti-P-glycoprotein (anti-MDR1, P7965) antibody, anti-Pin-1 mouse monoclonal antibody (WH0005300M1) were purchased from Sigma-Aldrich (USA). Dimethyl sulfoxide (DMSO) (1029521000) and chloroform (1070242500) were purchased from Merck (USA). 1,2-Distearoyl-sn-glycero-3-phosphoethanolamine-N-[amino (polyethylene glycol)-2000] (ammonium salt) (DSPE-PEG) (880128P) and Mini-Extruder were purchased from Avanti (USA). SPR gold-coated surfaces and QCM gold-coated surfaces (QSX301) were purchased from Reichert (USA) and Q-Sense (Sweden), respectively. In AFM imaging experiments, Nanosensors™ cantilevers (Model: PPP-NCHAuD; Force constant (k): 42N/m; Resonance Frequency (f): 328kHz, Switzerland) were used.

2.2. Preparation of MDR1-free and MDR1-incorporated liposomes

In protein-free liposome production, 100 μ L of PC solution (1 mg/mL in chloroform) was added into a round bottom flask (100 mL), and the flask was rotated under N₂ atmosphere. Thin lipid film was hydrated by adding phosphate buffer saline (PBS, 5 mL, 0.1 M, pH 7.4), and the solution was vortexed vigorously. This suspension was then extruded (Avanti Mini-Extruder) through a polycarbonate filter membrane with 100 nm pore size at least 15 times to obtain protein-free liposomes [35].

For protein-loaded liposome production, MDR1 stock solution was first prepared according to the manufacturer's protocol. Briefly, MDR1 protein solution (10 μ L) was added to 1 mL of EGTA-Tris buffer (0.1 M, pH 7.0), and the solution was stored at -20 °C for further use. For the production of MDR1 protein-loaded liposome, the same procedure in the protein-free liposome production was followed, and different volumes of MDR1 stock solution (0.7–5.0 μ L or 0.00014–0.001 (v:v)) was added to PBS before the extrusion step. As indicated by the manufacturer, Avanti Mini-Extruder System provides liposomes ranging from 120 to 140 nm. Further, MDR1 has two jut-outs (up-side: ~2 nm and down-side: ~8.6 nm) at membrane surface as reported in the literature [36].

2.3. Construction of tBLMs

Formation of tBLMs was performed in three steps: (i) activation of gold-coated surface (Fig. 1A), (ii) attachment of the tethering layer (B), and (iii) formation of either MDR1-free (C) or MDR1-integrated lipid bilayer (D). Gold-coated surfaces were activated with DTSP (1 mM in DMSO) at room temperature overnight, then washed with acetone, and dried with N₂ gas. The activated surfaces (Fig. 1A) were mounted to either SPR or QCM-D, and the system was stabilized using degassed distilled water. To construct the spacer layer, DSPE-PEG molecule was used at various concentrations (0.01–0.06 mg/mL in distilled water) (Fig. 1B). The system was then equilibrated with PBS, and either MDR1-free (Fig. 1C) or MDR1-incorporated liposome solution (D) was pumped through the reaction chamber until signal was stabilized. Unbound or weakly bound lipid vesicles were rinsed with PBS, and whole procedure was monitored by SPR and/or QCM-D.

2.4. Characterization of tBLMs

In SPR measurements, Reichert SR7000 SPR system (USA) and sensor chips (chromium (1 nm) and gold (50 nm) coated BK7 glass slides) were used. Refractive index changes were measured as micro refractive index unit (μ RIU) in 3 s. intervals (sensitivity: 0.75 μ RIU). In QCM-D (KSV QCM Z500, Finland) characterization, changes in frequency (f) and dissipation (D) were simultaneously monitored at 15, 25, 35, 45 MHz with different overtone values from 1 to 9. In these measurements, temperature was set to 25 °C, and the flow rate for all solutions was adjusted to 0.1 mL/min in both systems with a peristaltic pump (Masterflex Model 7550-50, USA). In AFM studies, NanoMagnetics Instruments AQUA non-contact-AFM system (Turkey) was used.

2.5. Antibody binding studies

To confirm the integration of MDR1 protein in tBLM platform, anti-MDR1 monoclonal antibody was used, and the binding events were monitored by SPR. To evaluate non-specific binding, anti-MDR1 antibody was also incubated with MDR1-free lipid bilayers. As a negative control, anti-Pin-1 (G8) monoclonal antibody was applied to the MDR1-integrated membrane platform. In these experiment, antibodies were diluted to 1:1000 (v:v) ratio with PBS, and then, introduced to the system. When the signal was stabilized, PBS was passed through the

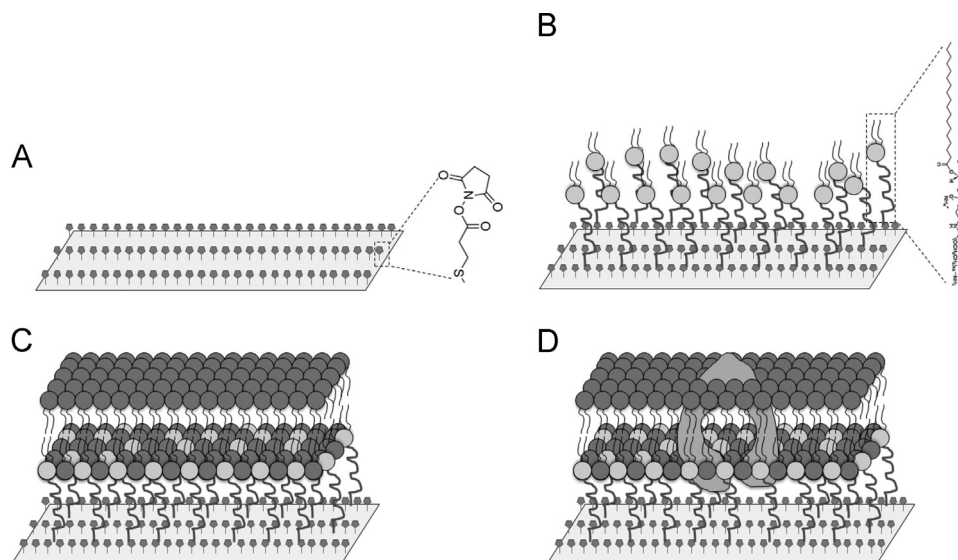


Fig. 1. Construction of tBLM on gold-coated surface. (A) Activation of the surface with DTSP. (B) DSPE-PEG modification. (C) Construction of protein-free tBLM. (D) Construction of protein-incorporated tBLM (molecules were not presented in their actual sizes).

system for rinsing till the signal was stabilized again.

2.6. Analysis of statin–MDR1 Interaction

For the demonstration of drug–membrane protein interaction, pravastatin (0.01 and 0.05 mg/mL in 0.1 M, pH: 7.4 PBS) was used. Drug solutions were circulated through SPR reaction chamber until the signal was stabilized, and then, washed with PBS. As a control experiment, 0.05 mg/mL of pravastatin was introduced MDR1-free membranes, and the same procedure was followed.

2.7. Statistical analysis

To assess the conformational transition of DSPE-PEG molecule from the mushroom to brush-like regime, the experimental results ($n=3$) were analyzed using analysis of variance (ANOVA) with Bonferroni correction for multiple comparisons ($p < 0.01$). To evaluate the effect of spacer concentration on liposome behavior, the experimental results ($n=3$) were analyzed using ANOVA with Tukey's post-hoc test for multiple comparisons ($p < 0.01$). To evaluate the effect of MDR1 amount on liposomal behavior, the experimental results ($n=3$) were analyzed using ANOVA with Tukey's post-hoc test for multiple comparisons ($p < 0.05$). All statistical analyses were performed using Minitab Software (Release 14; Minitab Inc, State College, PA).

3. Results and discussion

3.1. Characterization of DSPE-PEG layer

To construct a tBLM platform for the incorporation of transmembrane proteins with large hydrophilic domains, DSPE-PEG was used as a spacer molecule to elevate lipid bilayer. SPR results indicated that the μ RIU values increased with increasing DSPE-PEG concentrations (Fig. S1A). The lowest spacer concentration (0.01 mg/mL) presented a significantly lower μ RIU value compared to higher concentrations. After this transition, only a gradual increase was observed. QCM–D measurements presented consistent results with SPR experiments (Fig. S1B). Statistical analyses demonstrated that signal change in 0.02 mg/mL of spacer concentrations was significantly greater than that of 0.01 mg/mL for

both SPR (Fig. S1C) and QCM–D ($p < 0.01$) (D). Since dissipation is a vital parameter to understand this structural transition, especially affecting on viscoelastic properties of layers [37–39], the change in dissipation value was also evaluated, and a similar increase was also observed in these measurements (Fig. S1E). In our platform, viscoelastic property, molecular conformation and binding events are significantly affected by a long PEG chain ((OCH₂CH₂)₄₅) rather than lipid molecules (DSPE) in this hybrid spacer molecule. As reported in the literature, surface coverage of PEG molecules affects its conformation [33,39]. When the coverage is low, the distance between individual molecules restricts the intermolecular interactions. The intramolecular interactions are then favored, and a more compact conformation demonstrates a “mushroom-like” structure. On the other hand, at higher surface coverage, PEG residues starts to interact with each other that lead to a “brush-like” conformation, in which polymeric chains are extended from the surface. In our study, this transition was observed between 0.01 and 0.02 mg/mL of DSPE-PEG concentration.

3.2. The effect of DSPE-PEG concentration on liposome binding/spreading

A fixed concentration of liposome solution was incubated on tethered layers, which were prepared with different DSPE-PEG concentrations. Thus, the effect of DSPE-PEG concentrations on liposome binding/spreading was evaluated. In SPR measurements, DSPE-PEG amount on the surface significantly affected the behavior of liposome to form a lipid layer.

Statistical analyses on μ RIU values demonstrated that 0.03 and 0.04 mg/mL of DSPE-PEG concentrations were significantly greater than the other DSPE-PEG concentrations ($p < 0.01$) (Fig. S2A). In QCM–D frequency experiments, low DSPE-PEG concentrations (0.01 and 0.02 mg/mL) indicated that liposomes could not bind effectively on the tethered layer (Fig. S2B). Higher DSPE-PEG concentrations (0.04–0.06 mg/mL) implied different binding curves (data not shown) but the signal levels for these concentrations reverted to the starting level after washing step (Fig. S2B). Statistical analysis indicated that 0.03 mg/mL of DSPE-PEG concentration allowed significantly higher binding of liposomes compared to the other concentrations. Since both SPR and QCM–D experiments demonstrated that 0.03 mg/mL of DSPE-PEG concentration provided the highest binding level, further characterization experiments were continued

to carry out with this spacer concentration. Overall, 0.03 mg/mL of spacer concentration resulted in 1968 ± 126 μ RIU of a signal increase in SPR measurements, and 489 ± 91 Hz of a signal decrease in QCM frequency measurements.

Further, dissipation parameter of QCM–D measurements was assessed to determine the viscoelastic properties of the lipid layers. In the literature, $-\Delta D/\Delta f$ ratio was utilized to understand liposomal behavior on model membrane systems [39–42]. Briefly, high water content increases elasticity when the liposomes remain to be intact on the surface, and so, this event results in high $-\Delta D/\Delta f$ value. When liposomes fuse, deform and lose their water content by deformation, a more rigid layer is formed onto the surface and thus, $-\Delta D/\Delta f$ value decreases. As reported previously [43,44], the frequency value was first normalized using the overtone number, and then, the actual dissipation value was used in calculations. To compare these values, the exact dissipation and frequency values in the same overtone number was used. $-\Delta D/\Delta f$ ratios had been used to predict liposome behavior and bilayer formation on rigid membranes in the literature [44], in our case, however, liposomes were spread on top of a polymer-based spacer molecule, thus forming a viscoelastic layer. For this reason, the calculated values (Table 1) were used to comment on the relative rigidity of the constructed layers. As a result, high (0.04 and 0.06 mg/mL) and low (0.01 and 0.02 mg/mL) spacer concentrations resulted in high $-\Delta D/\Delta f$ ratios (between 3 and 6). As a measurement of rigid surface [44,45], Bovine Serum Albumin (BSA) was introduced to the sensor surface and $-\Delta D/\Delta f$ value of 1.3 ± 0.76 Hz was observed compared to 1.85 ± 0.15 Hz obtained by spacer concentration of 0.03 mg/mL. Therefore, it could be said that at 0.03 mg/mL of DSPE-PEG, liposome deformation, flattening and bilayer formation were observed more successfully compared to other concentrations. It should also be noted that mushroom to brush transition for the spacer layer was in between 0.01–0.02 mg/mL and 0.03 mg/mL just above the concentration where the intermolecular interactions started between individual chains but the surface coverage is relatively low. When spacer concentration was further increased, individual spacer chains would start to extend, and the height of the layer would increase. This might have an effect on the liposomal behavior on the surface. Overall, the polymer concentration and conformation played a key role in liposomal behavior and lipid bilayer construction.

Additionally, the mass load on the sensor surface were calculated using Sauerbrey's equation [46]. This formula correlates the decrease in frequency with the bound mass:

$$\Delta f = \frac{-2f_0^2 \Delta m}{\sqrt{\rho_q \mu_q}} \quad (1)$$

where f_0 is the resonance frequency of quartz crystal (Hz), μ_q is the shear modulus of quartz (2.947×10^{11} g cm⁻¹ s⁻²), ρ_q is the density of quartz (2.648 g cm⁻³), and Δm is the change in the bound mass per area (g cm⁻²). The following equation was also derived for the mass load calculations:

$$\Delta m = \frac{-C \Delta f}{n} \quad (2)$$

where C is the mass sensitivity constant (17.7 ng cm⁻² Hz⁻¹ for $f=5$ MHz crystals), and n is the overtone number (3, 5, ..., n).

Mass load is dependent on several parameters including layer characteristics (e.g., rigidity and viscoelasticity) and sensor properties (e.g., resonance frequency, shear modulus, and the density of quartz). Theoretical calculations demonstrated a ~ 2.1 μ g/cm² of mass accumulation by considering molecular weight and head group size of PC molecules [44,47]. In optimum conditions (0.03 mg/mL of spacer concentration), the constructed layer resulted in a 1.2 ± 0.3 μ g/cm² of mass load. In the literature, there are rigid lipid bilayer platforms reported with a mass load ranging from ~ 400 to ~ 500 ng/cm² using the Sauerbrey model [43,48,49]. Considering these values, the mass load in our platform is three times higher than the Sauerbrey model-based studies. However, this model is valid in acoustically rigid films with low dissipation [47,50], and it is insufficient when ΔD is more than zero [51]. In our platform, on the other hand, the polymer-based spacer layer provides a viscoelastic layer. In the literature, the Voigt–Voinova model is described to measure the changes in mass

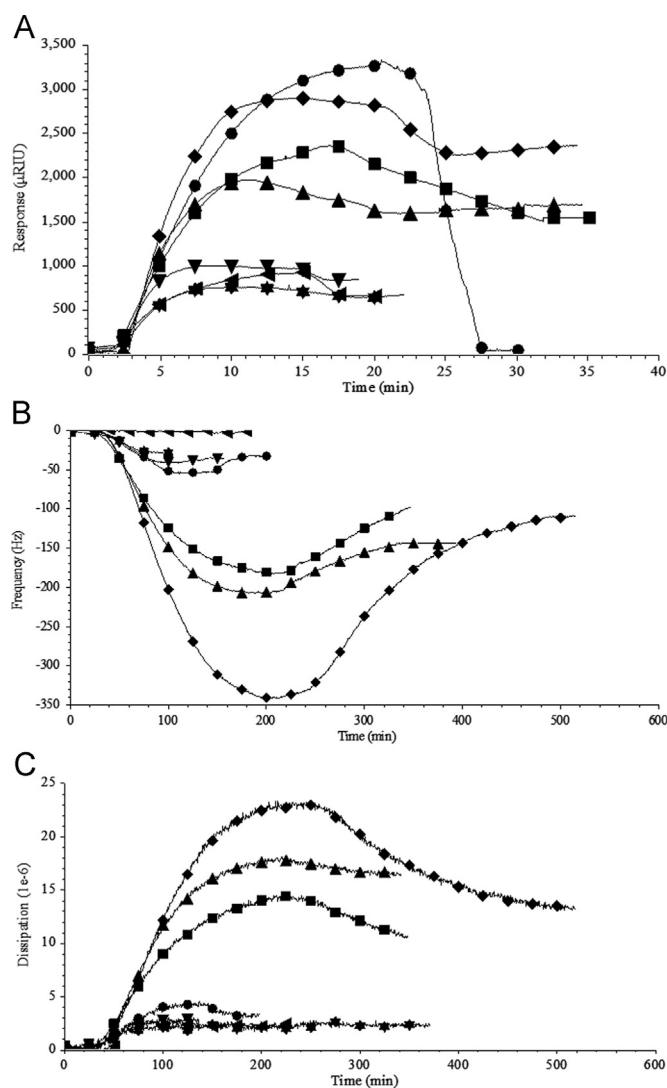


Fig. 2. Binding and spreading of MDR1-incorporated liposomes at various MDR1 volumes on 0.03 mg/mL of DSPE-PEG-modified surfaces by (A) SPR (\bullet 0.7; \blacksquare 0.9; \blacklozenge 1.0; \blacktriangle 2.0; \blacktriangledown 3.0; \ast 4.0; \blacktriangleleft 5.0 μ L of MDR1) and QCM–D (\bullet 0.7; \blacksquare 0.8; \blacklozenge 0.9; \blacktriangle 1.0; \blacktriangledown 2.0; \ast 3.0; \blacktriangleleft 4.0 μ L of MDR1) (overtone number: 7), (B) using frequency and (C) dissipation parameters.

Table 1
Effect of DSPE-PEG concentration on the behavior of liposomes on the surface.

DSPE-PEG concentration (mg/mL)	$-\Delta D/\Delta f$ ratio
0.01	4.03 ± 3.53
0.02	5.71 ± 1.13
0.03	1.85 ± 0.15
0.04	6.16 ± 2.58
0.05	5.20 ± 0.61
0.06	3.38 ± 1.20

and effective viscoelastic features of the layer during the transformation process from adsorbed vesicles to a lipid bilayer [50,52,53]. The additional mass of coupled water associated with the spacer layer has been demonstrated to change significantly in different platforms, depending on the nature of the spacer layer. A mass uptake between 1.5 and 10 times higher than the mass of the adsorbed material was generally estimated [53,54]. Similarly, a PEG spacer-based lipid bilayer system presented a mass load ranging from ~ 1.4 to $\sim 1.8 \mu\text{g}/\text{cm}^2$ by changing the spacer concentration whereas the dry mass ranges between ~ 0.16 and $\sim 0.2 \mu\text{g}/\text{cm}^2$ [10]. In our study, the polymer spacer provides a viscoelastic layer (*i.e.*, cushion-like structure) and considerably holds water, thus increasing the total mass three times higher than that of the rigid layer calculated by the Sauerbrey model. This excessive mass in our platform is comparable to the reported values in the literature, and it is also in the range of the estimated mass calculations (*i.e.*, 1.5–10 times higher than the rigid layers) in the Voigt–Voinova model. This difference implies that some of the liposomes were deformed and spontaneously fuse to either construct a lipid bilayer or form partial local multilayers [40,44,47,55,56].

3.3. The effect of MDR1 amount on liposome binding/spreading

Various volumes of MDR1 stock solution (0.7–5.0 μL or 0.00014–0.001 (v:v)) were evaluated to understand optimum MDR1 amount to construct a successful platform. SPR analysis demonstrated that liposomes with low (0.7 μL or 0.00014 (v:v)) and high (3.0–5.0 μL or 0.0006–0.001 (v:v)) MDR1 ratio were either fully removed from the surface or not efficiently bound to the surface (Fig. 2A). When liposomes prepared with 0.9–2.0 μL (0.00018–0.0004 (v:v)) of MDR1 stock solution were used, stable lipid layer was observed. In QCM–D frequency measurements, low (0.7 μL or 0.00014 (v:v)) and high (2.0–4.0 μL or 0.0004–0.0008 (v:v)) volumes of protein resulted in low binding capacity (Fig. 2B)

while 0.8–1.0 μL (*i.e.*, 0.0016–0.0002 (v:v)) resulted in more stable surfaces. Moreover, liposomes prepared with 1.0 μL (*i.e.*, 0.0002 (v:v)) of MDR1 stock solution resulted in surfaces with highest dissipation value (Fig. 2C). Statistical analyses indicated that the usage of 1 μL (*i.e.*, 0.0002 (v:v)) of MDR1 stock solution resulted in the construction of a protein-incorporated lipid layer with significantly higher values in both characterization experiments ($n=3$, $p < 0.05$) (Fig. S3).

QCM–D dissipation analysis showed that the presence of MDR1 protein caused a decrease in dissipation value, resulting in more rigid layers, and possibly hindrance in the movement of phospholipids as observed in their native environment [43,47,55], and possibly increased the stability of the platform by restricting phospholipid movement. The mass load caused by MDR1-incorporation was calculated as $1.67 \mu\text{g}/\text{cm}^2$, and thus, the total mass load increased *ca.* $0.47 \mu\text{g}/\text{cm}^2$ compared to MDR1-free lipid layers. In the literature, the protein insertion demonstrated a decrease in the efficiency of lipid bilayer construction, and to construct lipid bilayer, in some studies, the outward sections of the proteins were cleaved enzymatically and a truncated form of the protein was used [57]. In our tBLM platform, there is no need for enzymatic cleavage of the outward sections and the MDR1 was incorporated without any modification.

3.4. Visualization by Atomic Force Microscopy operating in liquids

Overall roughness of unmodified gold-coated BK7 surfaces (SPR sensor slides) was first measured as *ca.* 8 nm. High roughness value of BK7 surfaces might be caused from the abrasive machining processes (*e.g.*, cutting and shaping of glass slides) [58]. When optimum DSPE-PEG concentration (0.03 mg/mL) was used, a condensed structure with 0.39 nm of roughness was observed in the AFM studies (Fig. 3A). The spacer layer was further investigated with 6 nm of vertical scale to visualize the behavior of the spacer molecule (Fig. 3B). In this spacer concentration

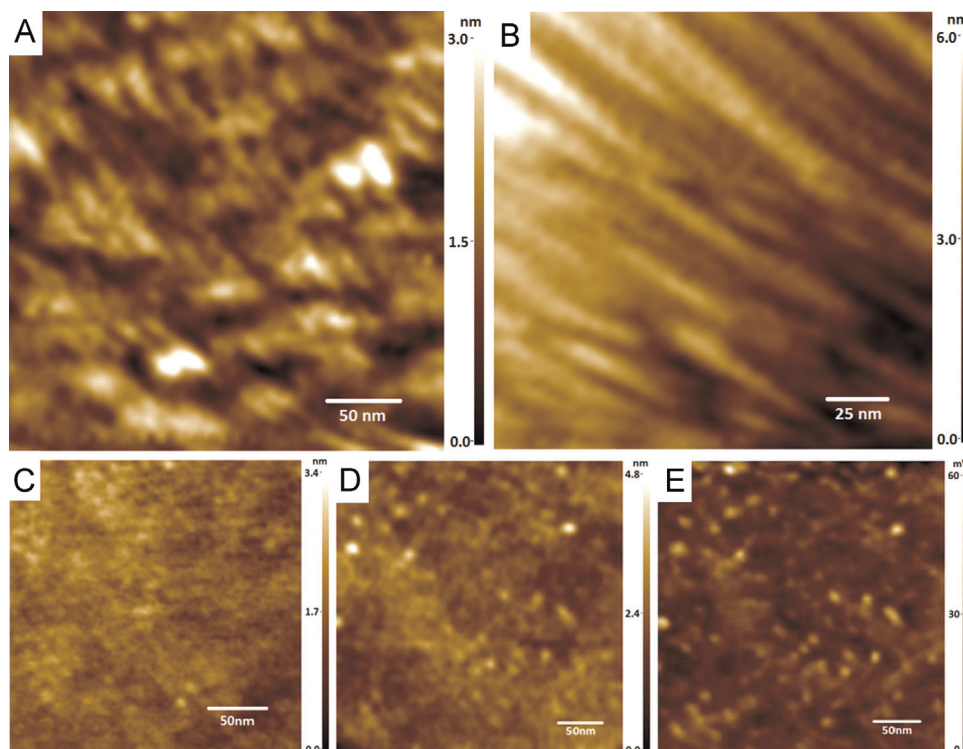


Fig. 3. Visualization of DSPE-PEG modified surface and liposome binding/spreading using AFM. Topography images of DSPE-PEG layer with (A) 3 nm and (B) 6 nm of vertical scale. Topography image of (C) MDR1-free tBLM and (D) MDR1-integrated tBLM. Dissipation image of (E) MDR1-integrated tBLM.

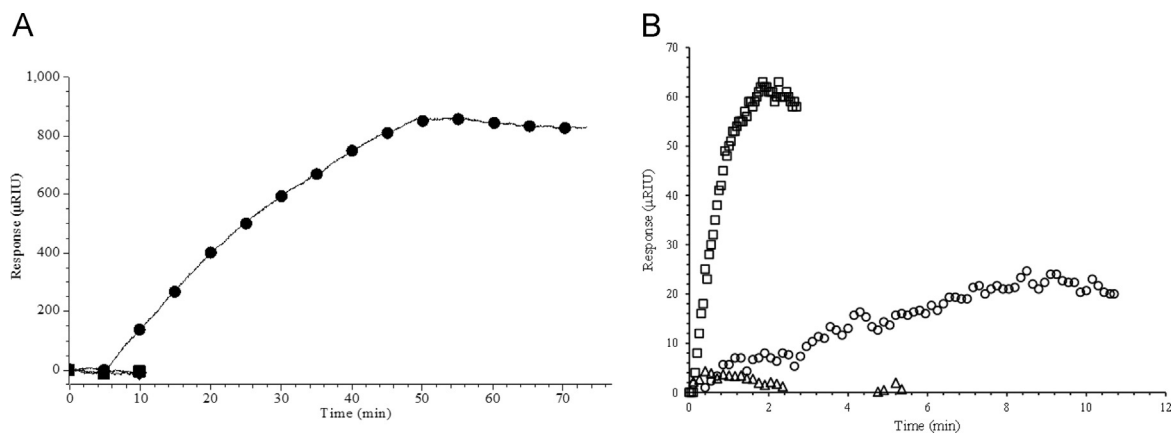


Fig. 4. Antibody and pravastatin binding on MDR1-incorporated tBLM by SPR. (A) (●) Binding result of anti-MDR1 monoclonal antibody on MDR1-incorporated tBLM. (■) Binding result of anti-MDR1 antibody on MDR1-free tBLM. (▲) Binding result of anti-Pin-1 (G8) mouse monoclonal antibody on MDR1-incorporated tBLM. (B) Binding result of (○) 0.05 mg/mL and (◻) 0.01 mg/mL pravastatin solutions on MDR1-incorporated tBLM and binding of 0.05 mg/mL of pravastatin (△) on MDR1-free bilayers.

(0.03 mg/mL), intermolecular interactions between PEG residues appeared to be critical, and “brush-like” conformation, in which thin and long polymeric chains extended through vertical direction, was observed in the AFM analysis [59–61]. Further, this directional behavior was not observed in surfaces with lower DSPE-PEG coverage such as 0.0003 mg/mL, probably due to the occurrence of “mushroom like” structure explained in previous sections.

Additionally, DSPE-PEG layer was investigated after drying in air for 24 h, and a highly rough surface (ca. 15 nm) was observed (Fig. S4B) as opposed to measurements under aqueous conditions (A). After re-hydration with PBS and incubation for 3 h, smooth and uniform coating was regenerated as observed previously (Fig. S4C). Thus, re-hydration allowed spreading of the liposomes. This structural regeneration offered a great opportunity to dry and store the spacer layer until it was used for further modifications.

After the application of liposomes onto the DSPE-PEG layer, the roughness did not alter significantly, and a flat surface with 0.45 nm of roughness was measured using AFM system (Fig. 3C). In literature, the height of lipid bilayer was reported as ca. 3–4 nm [36], and well-organized lipid bilayer was theoretically expected to be smooth. As observed in QCM–D measurements, AFM also indicated that the most of liposomes were deformed and fused to form either a lipid bilayer or partially local multilayers on the surface. The presence of MDR1 proteins increased the roughness value to 1.23 nm (Fig. 3D). Small region scans on the topography imaging typically demonstrated several jut-outs with ca. 1.5 nm on the platform (Fig. 3D). The presence of jut-outs becomes more pronounced in dissipation image (E); stiff regions spread to comparatively more viscoelastic areas on the surface were observed, and these stiff regions was thought to indicate the proteins incorporated into the lipid bilayer platform.

3.5. Antibody binding analysis

Anti-MDR1 human monoclonal antibody against extracellular site of MDR1 protein was used to evaluate the orientation and presence of MDR1 protein in lipid bilayers. Anti-MDR1 antibody caused a 841 ± 20 μ RIU change (Fig. 4A). In addition, two different control sets were utilized to demonstrate the specificity of antibody binding to MDR1-incorporated lipid bilayer. No binding was observed when anti-MDR1 antibody was interacted with MDR1-free lipid layers. Anti-Pin-1 (G8) mouse monoclonal antibody, which is known to have no interaction with MDR1 protein, also showed no binding (Fig. 4A). Thus, antibody analysis demonstrated that MDR1 protein was inserted into the lipid bilayers.

3.6. Analysis of statin–MDR1 interactions

For the preliminary investigation to evaluate the potential of the platform in membrane protein–drug interactions, a statin-based molecule, pravastatin was applied onto MDR1-loaded lipid bilayer system. Since the stability of lipid layer was affected by organic solvents, more hydrophobic statin molecules (*i.e.*, lovastatin and simvastatin) require organic solvent usage, and could not be applied to the membrane platform. Two different concentrations (0.01 and 0.05 mg/mL) of pravastatin resulted in ~ 20 and 60 μ RIU, respectively (Fig. 4B). At lower pravastatin concentrations (< 0.01 mg/mL), the signal remained on the noise level. There was no significant signal observed when pravastatin was incubated with MDR1-free membranes (Fig. 4B). In sum, the interactions between pravastatin and MDR1 proteins were demonstrated on the model membrane system.

4. Conclusion

In this study, a tBLM platform was constructed using a long spacer molecule (*i.e.*, DSPE-PEG) for the incorporation of MDR1, a transmembrane protein with large extra-membrane domain. Here, spacer concentration significantly affected the behavior of liposomes on the surface. Incorporation of MDR1 resulted in more rigid layers as shown by QCM–D and AFM results. Constructed platform enabled to directly examine drug–membrane protein interactions by introducing pravastatin to MDR1-integrated lipid membranes. In sum, this presented study offers an alternative approach to investigate membrane protein characteristics and drug–membrane protein interactions without any considerable damage on native structure of membrane proteins. Additionally, in the future, this platform can be potentially integrated with distinct modalities such as plasmonic [62], photonic [63], electrical [64] and nanomechanical systems [65]. Further, it can be deployed to microfluidics [66], lab-on-a-chip systems [67], drug delivery [68] and biosensor platforms [69] to investigate potential interactions of several drugs with various membrane proteins *in vitro* conditions, as well as to monitor binding events in molecular levels.

Acknowledgments

The authors would like to thank TUBITAK to The Scientific and Technological Research Council of Turkey (TUBITAK) (108T933) for providing financial support. A part of the study was supported by

ITU-BAP (33620, 33146). FI acknowledges Ph.D. scholarship from TUBITAK.

Appendix A. Transparency document

Transparency document associated with this article can be found in the online version at <http://dx.doi.org/10.1016/j.bbrep.2015.05.012>.

Appendix B. Supplementary material

Supplementary material associated with this article can be found in the online version at <http://dx.doi.org/10.1016/j.bbrep.2015.05.012>.

References

- [1] R. Arnell, N. Ferraz, T. Fornstedt, Analytical characterization of chiral drug–protein interactions: comparison between the optical biosensor (surface plasmon resonance) assay and the HPLC perturbation method, *Anal. Chem.* 78 (5) (2006) 1682–1689.
- [2] J.A. Jackman, W. Knoll, N.-J. Cho, Biotechnology applications of tethered lipid bilayer membranes, *Materials* 5 (12) (2012) 2637–2657.
- [3] J. Struppe, J.A. Whiles, R.R. Vold, Acidic phospholipid bicelles: a versatile model membrane system, *Biophys. J.* 78 (1) (2000) 281–289.
- [4] T.H. Bayburt, S.G. Sligar, Membrane protein assembly into nanodiscs, *FEBS Lett.* 584 (9) (2010) 1721–1727.
- [5] M. Lucio, H. Ferreira, J.L.F.C. Lima, S. Reis, Use of liposomes as membrane models to evaluate the contribution of drug–membrane interactions to anti-oxidant properties of etodolac, *Redox Rep.* 13 (5) (2008) 225–236.
- [6] M. Winterhalter, Black lipid membranes, *Curr. Opin. Colloid Interface Sci.* 5 (3) (2000) 250–255.
- [7] R.P. Richter, J.L.K. Him, A. Brisson, Supported lipid membranes, *Mater. Today* 6 (11) (2003) 32–37.
- [8] E.-K. Sinner, U. Reuning, F.N. Kök, B. Saccà, L. Moroder, W. Knoll, D. Oesterhelt, Incorporation of integrins into artificial planar lipid membranes: characterization by plasmon-enhanced fluorescence spectroscopy, *Anal. Biochem.* 333 (2) (2004) 216–224.
- [9] F. Giess, M.G. Friedrich, J. Heberle, R.L. Naumann, W. Knoll, The protein-tethered lipid bilayer: a novel mimic of the biological membrane, *Biophys. J.* 87 (5) (2004) 3213–3220.
- [10] A. Coutable, C. Thibault, J. Chalmeau, J.M. François, C. Vieu, V. Noireaux, E. Trévisiol, Preparation of tethered-lipid bilayers on gold surfaces for the incorporation of integral membrane proteins synthesized by cell-free expression, *Langmuir* 30 (11) (2014) 3132–3141.
- [11] S. Hertrich, F. Stetter, A. Rühm, T. Hugel, B. Nickel, Highly hydrated deformable polyethylene glycol-tethered lipid bilayers, *Langmuir* 30 (31) (2014) 9442–9447.
- [12] A. Janshoff, C. Steinem, Transport across artificial membranes—an analytical perspective, *Anal. Bioanal. Chem.* 385 (3) (2006) 433–451.
- [13] R. Naumann, S.M. Schiller, F. Giess, B. Grohe, K.B. Hartman, I. Koper, J. Lubben, K. Vasilev, W. Knoll, Tethered lipid bilayers on ultraflat gold surfaces, *Langmuir* 19 (13) (2003) 5435–5443.
- [14] S.M. Schiller, R. Naumann, K. Lovejoy, H. Kunz, W. Knoll, Archaea analogue thiolipids for tethered bilayer membranes on ultrasmooth gold surfaces, *Angew. Chem.—Int. Ed.* 42 (2) (2003) 208.
- [15] J. Homola, Surface plasmon resonance sensors for detection of chemical and biological species, *Chem. Rev.* 108 (2) (2008) 462–493.
- [16] M. Hoepfner, U. Rothe, G. Bendas, Biosensor-based evaluation of liposomal behavior in the target binding process, *J. Liposome Res.* 18 (1) (2008) 71–82.
- [17] E. Briand, M. Zach, S. Svedhem, B. Kasemo, S. Petronis, Combined QCM-D and EIS study of supported lipid bilayer formation and interaction with pore-forming peptides, *Analyst* 135 (2) (2010) 343–350.
- [18] P.-E. Milhiet, F. Gubellini, A. Berquand, P. Dossat, J.-L. Rigaud, C. Le Grimallec, D. Levy, High-resolution AFM of membrane proteins directly incorporated at high density in planar lipid bilayer, *Biophys. J.* 91 (9) (2006) 3268–3275.
- [19] M.F. Fromm, P-glycoprotein: a defense mechanism limiting oral bioavailability and CNS accumulation of drugs, *Int. J. Clin. Pharmacol. Ther.* 38 (2) (2000) 69–74.
- [20] B.L. Neudeck, J.M. Loeb, N.G. Faith, C.J. Czuprynski, Intestinal P glycoprotein acts as a natural defense mechanism against *Listeria monocytogenes*, *Infect. Immunology* 72 (7) (2004) 3849–3854.
- [21] I. Ieiri, Functional significance of genetic polymorphisms in P-glycoprotein (MDR1, ABCB1) and breast cancer resistance protein (BCRP, ABCG2), *Drug Metab. Pharmacokinet.* 27 (1) (2012) 85–105.
- [22] H. He, K. Lyons, X. Shen, Z. Yao, K. Bleasby, G. Chan, M. Hafey, X. Li, S. Xu, G. Salituro, Utility of unbound plasma drug levels and P-glycoprotein transport data in prediction of central nervous system exposure, *Xenobiotica* 39 (9) (2009) 687–693.
- [23] G.J. Anger, A.M. Cressman, M. Piquette-Miller, Expression of ABC efflux transporters in placenta from women with insulin-managed diabetes, *PloS One* 7 (4) (2012) e35027.
- [24] F. Falasca, P. Maida, C. Montagna, L. Antonelli, G. d’Ettorre, K. Monteleone, G. Antonelli, O. Turriziani, Expression of the mRNA levels for MDR1, MRP1, MRP4, and MRP5 in HIV antiretroviral naive patients: follow-up at 48 weeks after the beginning of therapy, *J. Acquir. Immune Defic. Syndr.* 56 (2) (2011) e54–e56.
- [25] L. He, J.W. Robertson, J. Li, I. Kärcher, S.M. Schiller, W. Knoll, R. Naumann, Tethered bilayer lipid membranes based on monolayers of thiolipids mixed with a complementary dilution molecule. 1. Incorporation of channel peptides, *Langmuir* 21 (25) (2005) 11666–11672.
- [26] V. Atanasov, N. Knorr, R.S. Duran, S. Ingebrandt, A. Offenhäuser, W. Knoll, I. Köper, Membrane on a chip: a functional tethered lipid bilayer membrane on silicon oxide surfaces, *Biophys. J.* 89 (3) (2005) 1780–1788.
- [27] M.L. Wagner, L.K. Tamm, Tethered polymer-supported planar lipid bilayers for reconstitution of integral membrane proteins: silane-polyethyleneglycol-lipid as a cushion and covalent linker, *Biophys. J.* 79 (3) (2000) 1400–1414.
- [28] J.C. Munro, C.W. Frank, In situ formation and characterization of poly (ethylene glycol)-supported lipid bilayers on gold surfaces, *Langmuir* 20 (24) (2004) 10567–10575.
- [29] Y.-H. Lin, D.E. Minner, V.L. Herring, C.A. Naumann, Physisorbed polymer-tethered lipid bilayer with lipopolymer gradient, *Materials* 5 (11) (2012) 2243–2257.
- [30] O. Purrucker, A. Förtig, R. Jordan, M. Tanaka, Supported membranes with well-defined polymer tethers—incorporation of cell receptors, *ChemPhysChem* 5 (3) (2004) 327–335.
- [31] W. Knoll, C. Frank, C. Heibel, R. Naumann, A. Offenhäuser, J. Rühle, E. Schmidt, W. Shen, A. Sinner, Functional tethered lipid bilayers, *Rev. Mol. Biotechnol.* 74 (3) (2000) 137–158.
- [32] M. Wallin, J.-H. Choi, S. Kim, N.-J. Cho, M. Andersson, Peptide-induced formation of a tethered lipid bilayer membrane on mesoporous silica, *Eur. Biophys. J.* 44 (1–2) (2015) 27–36.
- [33] S. Kaufmann, O. Borisov, M. Textor, E. Reimhult, Mechanical properties of mushroom and brush poly (ethylene glycol)–phospholipid membranes, *Soft Matter* 7 (19) (2011) 9267–9275.
- [34] E.J. Wang, C.N. Casciano, R.P. Clement, W.W. Johnson, HMG-CoA reductase inhibitors (statins) characterized as direct inhibitors of P-glycoprotein, *Pharm. Res.* 18 (6) (2001) 800–806.
- [35] L. Martini, S.S. Mansy, Cell-like systems with riboswitch controlled gene expression, *Chem. Commun.* 47 (38) (2011) 10734–10736.
- [36] Karasu, D., Bir membran proteini olan P-glikoproteinini statin bazlı kolesterol düşürücü ilaçlarla etkileşiminin moleküler modelleme yoluyla incelenmesi. in: *Molecular Biology—Genetics and Biotechnology*. Istanbul Technical University, 2011.
- [37] N. Srinivasan, M. Bhagwati, B. Ananthanarayanan, S. Kumar, Stimuli-sensitive intrinsically disordered protein brushes, *Nat. Commun.* 5 (2014).
- [38] Y. Hu, J. Jin, Y. Han, J. Yin, W. Jiang, H. Liang, Study of fibrinogen adsorption on poly (ethylene glycol)-modified surfaces using a quartz crystal microbalance with dissipation and a dual polarization interferometry, *RSC Adv.* 4 (15) (2014) 7716–7724.
- [39] J. Lin, J. Szymanski, P.C. Searson, K. Hristova, Effect of a polymer cushion on the electrical properties and stability of surface-supported lipid bilayers, *Langmuir* 26 (5) (2009) 3544–3548.
- [40] M. Hopfner, U. Rothe, G. Bendas, Biosensor-based evaluation of liposomal behavior in the target binding process, *J. Liposome Res.* 18 (1) (2008) 71–82.
- [41] E. Reimhult, F. Hook, B. Kasemo, Vesicle adsorption on SiO₂ and TiO₂: dependence on vesicle size, *J. Chem. Phys.* 117 (16) (2002) 7401–7404.
- [42] T.R. Khan, H.M. Grandin, A. Mashaghi, M. Textor, E. Reimhult, I. Reviakine, Lipid redistribution in phosphatidylserine-containing vesicles adsorbing on titania, *Biointerphases* 3 (2) (2008) FA90.
- [43] C.A. Keller, B. Kasemo, Surface specific kinetics of lipid vesicle adsorption measured with a quartz crystal microbalance, *Biophys. J.* 75 (3) (1998) 1397–1402.
- [44] G. Bendas, Biosensor-based evaluation of liposomal binding behavior, *Methods Mol. Biol.* 606 (2010) 519–529.
- [45] Q. Ye, R. Konradi, M. Textor, E. Reimhult, Liposomes tethered to omega-functional PEG brushes and induced formation of PEG brush supported planar lipid bilayers, *Langmuir* 25 (23) (2009) 13534–13539.
- [46] G. Sauerbrey, Verwendung von Schwingquarzen zur Wägung dünner Schichten und zur Mikrowägung, *Z. Phys. A Hadrons Nucl.* 155 (2) (1959) 206–222.
- [47] E. Reimhult, F. Hook, B. Kasemo, Intact vesicle adsorption and supported biomembrane formation from vesicles in solution: influence of surface chemistry, vesicle size, temperature, and osmotic pressure, *Langmuir* 19 (5) (2003) 1681–1691.
- [48] R. Richter, A. Mukhopadhyay, A. Brisson, Pathways of lipid vesicle deposition on solid surfaces: a combined QCM-D and AFM study, *Biophys. J.* 85 (5) (2003) 3035–3047.
- [49] K.O. Evans, Supported phospholipid bilayer interaction with components found in typical room-temperature ionic liquids—a QCM-D and AFM study, *Int. J. Mol. Sci.* 9 (4) (2008) 498–511.
- [50] N.-J. Cho, C.W. Frank, B. Kasemo, F. Höök, Quartz crystal microbalance with

- dissipation monitoring of supported lipid bilayers on various substrates, *Nat. Protoc.* 5 (6) (2010) 1096–1106.
- [51] D.J. Silva, O.J. Rojas, S.W. Park, M.A. Hubbe, Evaluation of adsorbed poly-ampholyte layers by using quartz crystal microbalance, *Comput. Aided Chem. Eng.* 27 (2009) 1929–1934.
- [52] M.V. Voinova, M. Rodahl, M. Jonson, B. Kasemo, Viscoelastic acoustic response of layered polymer films at fluid–solid interfaces: continuum mechanics approach, *Phys. Scr.* 59 (5) (1999) 391.
- [53] F. Höök, B. Kasemo, T. Nylander, C. Fant, K. Sott, H. Elwing, Variations in coupled water, viscoelastic properties, and film thickness of a Mefp-1 protein film during adsorption and cross-linking: a quartz crystal microbalance with dissipation monitoring, ellipsometry, and surface plasmon resonance study, *Anal. Chem.* 73 (24) (2001) 5796–5804.
- [54] N.-J. Cho, K.K. Kanazawa, J.S. Glenn, C.W. Frank, Employing two different quartz crystal microbalance models to study changes in viscoelastic behavior upon transformation of lipid vesicles to a bilayer on a gold surface, *Anal. Chem.* 79 (18) (2007) 7027–7035.
- [55] E. Reimhult, M. Zach, F. Hook, B. Kasemo, A multitechnique study of liposome adsorption on Au and lipid bilayer formation on SiO₂, *Langmuir* 22 (7) (2006) 3313–3319.
- [56] J.J. Stalgren, P.M. Claesson, T. Warnheim, Adsorption of liposomes and emulsions studied with a quartz crystal microbalance, *Adv. Colloid Interface Sci.* 89–90 (2001) 383–394.
- [57] A. Graneli, J. Rydstrom, B. Kasemo, F. Hook, Formation of supported lipid bilayer membranes on SiO₂ from proteoliposomes containing transmembrane proteins, *Langmuir* 19 (3) (2003) 842–850.
- [58] D. Lv, Y. Huang, Y. Tang, H. Wang, Relationship between subsurface damage and surface roughness of glass BK7 in rotary ultrasonic machining and conventional grinding processes, *Int. J. Adv. Manuf. Technol.* (2012) 1–10.
- [59] A.K. Kenworthy, K. Hristova, D. Needham, T.J. McIntosh, Range and magnitude of the steric pressure between bilayers containing phospholipids with covalently attached poly(ethylene glycol), *Biophys. J.* 68 (5) (1995) 1921–1936.
- [60] J.V. Jokerst, T. Lobovkina, R.N. Zare, S.S. Gambhir, Nanoparticle PEGylation for imaging and therapy, *Nanomedicine* 6 (4) (2011) 715–728.
- [61] C. Allen, N. Dos Santos, R. Gallagher, G.N. Chiu, Y. Shu, W.M. Li, S.A. Johnstone, A.S. Janoff, L.D. Mayer, M.S. Webb, M.B. Bally, Controlling the physical behavior and biological performance of liposome formulations through use of surface grafted poly(ethylene glycol), *Biosci. Rep.* 22 (2) (2002) 225–250.
- [62] F. Inci, O. Tokel, S. Wang, U.A. Gurkan, S. Tasoglu, D.R. Kuritzkes, U. Demirci, Nanoplasmonic quantitative detection of intact viruses from unprocessed whole blood, *ACS Nano* 7 (6) (2013) 4733–4745.
- [63] H. Shafiee, E.A. Lidstone, M. Jahangir, F. Inci, E. Hanhauser, T.J. Henrich, D. R. Kuritzkes, B.T. Cunningham, U. Demirci, Nanostructured optical photonic crystal biosensor for HIV viral load measurement, *Sci. Rep.* 4 (2014).
- [64] H. Shafiee, W. Asghar, F. Inci, M. Yuksekkaya, M. Jahangir, M.H. Zhang, N. G. Durmus, U.A. Gurkan, D.R. Kuritzkes, U. Demirci, Paper and flexible substrates as materials for biosensing platforms to detect multiple biotargets, *Sci. Rep.* 5 (2015).
- [65] C. Lissandrello, F. Inci, M. Francom, M. Paul, U. Demirci, K. Ekinici, Nano-mechanical motion of *Escherichia coli* adhered to a surface, *Appl. Phys. Lett.* 105 (11) (2014) 113701.
- [66] S. Wang, M. Esfahani, U.A. Gurkan, F. Inci, D.R. Kuritzkes, U. Demirci, Efficient on-chip isolation of HIV subtypes, *Lab Chip* 12 (8) (2012) 1508–1515.
- [67] S. Wang, F. Inci, T.L. Chaunzwa, A. Ramanujam, A. Vasudevan, S. Subramanian, A.C.F. Ip, B. Sridharan, U.A. Gurkan, U. Demirci, Portable microfluidic chip for detection of *Escherichia coli* in produce and blood, *Int. J. Nanomed.* 7 (2012) 2591.
- [68] C. Peetla, A. Stine, V. Labhasetwar, Biophysical interactions with model lipid membranes: applications in drug discovery and drug delivery, *Mol. Pharm.* 6 (5) (2009) 1264–1276.
- [69] Y.K. Lee, H. Lee, J.-M. Nam, Lipid–nanostructure hybrids and their applications in nanobiotechnology, *NPG Asia Mater.* 5 (5) (2013) e48.